

Tunneling through X -valley-related impurity states in GaAs/AlAs resonant-tunneling diodes

S. A. Vitusevich,* A. Förster, K. M. Indlekofer, and H. Lüth
Institut für Schicht- und Ionentechnik, Forschungszentrum Jülich, D-52425 Jülich, Germany

A. E. Belyaev, B. A. Glavin, and R. V. Konakova
Institute of Semiconductor Physics, National Academy of Sciences of Ukraine, Kiev 252028, Ukraine
(Received 6 July 1999)

We have investigated resonant tunneling through impurity states with large binding energy of the GaAs/AlAs double-barrier resonant tunneling heterostructure. These states originate due to the penetration of Si impurity atoms from the heavily doped emitter layer that is adjacent to one of the two AlAs layers. Magnetotunneling transport results demonstrate that resonant peaks and steps arise due to tunneling through the X -valley-related donor states localized in an AlAs layer. The strong asymmetry of the doping profile in our structures provides substantial accumulation of the resonant electrons at one bias polarity, which gives rise to the intrinsic bistability observed for the impurity-assisted resonant tunneling. Using perturbation theory, we estimated the value of the current and tunneling rates through the X -valley-related donor states, which is in good agreement with the measured current value and the registered bistability effect. Observed Zeeman splitting of the current peak allowed us to determine the value of the g factor of the confined impurity states.

INTRODUCTION

A resonant-tunneling diode (RTD), in addition to its promising applications in ultrahigh-speed electronics and optoelectronics, is an attractive object for the studies of quantum electron transport. Recent progress in multilayered structure growth technology has made it possible to observe, along with main resonant peaks arising from tunneling through the quasibound states of the well and demonstrated by a pioneering study of RTD,¹ numerous novel peculiarities in the tunneling current. New features in the current-voltage characteristics $I(V)$ provide useful information about phonon-² and plasmon-assisted tunneling³ and about coherent and inelastic mechanisms of tunneling through quantum-well (QW) states.⁴ The effect of intrinsic bistability has been observed and its origin was established as a charge buildup in the quantum well of the RTD or in the triangular quantum well of the accumulation layer formed in front of the emitter barrier region.⁵⁻⁷ Recently observed new peaks and steps in the prethreshold region of gated undoped RTD's attract growing interest.⁸ These features are explained by the presence of a hydrogenic impurity in the QW of the RTD. The impurity states usually have a binding energy⁹ of the order of 20 meV with respect to the bottom of the two-dimensional (2D) band in the QW. It has been suggested that impurities can diffuse from highly doped emitter regions and can create donor impurity levels in undoped QW's. An investigation of RTD's with intentionally doped QW's proved¹⁰ that impurities can create channels for resonant tunneling through the 0D impurity states. To observe quantum-mechanical tunneling through these localized states it is not necessary to have a small mesa size, as in the case of Coulomb blockade effects. At the same time, impurities control the electrical and optical properties of the RTD. An impurity-assisted tunneling mechanism can give rise to several well-resolved peaks in $I(V)$ characteristics that can be used in high-speed electronics. In addition, they provide useful information about

the electrostatic profile of the structure as well as about parameters of the impurity-related tunneling process. Important characteristics, such as the wave function of a shallow donor, may be deduced from the variation of the resonant peak amplitude with the magnetic field.¹¹ Recently observed spin splitting of the impurity level¹² in the RTD made it possible to obtain impurity-assisted tunneling rates in the structure.

Further experimental data¹³ show that some resonant peaks and steps are observed in very low voltage ranges and cannot be ascribed to single shallow donor states of the QW state. To explain this feature, a model was proposed, according to which coupling between the impurity states of different atoms leads to an increase of the impurity binding energy, which somewhat resembles the formation of hydrogen molecules from the solitary atoms. The authors of Ref. 14 developed an alternative model, where the high binding energy of impurities was explained by the fluctuations of the QW width.

In this work we present the results of studies of the impurity-assisted tunneling in strongly asymmetrically doped GaAs/AlAs RTD's. The results obtained permit us to conclude that the observed resonant transmissions in a very low voltage range are due to the tunneling through the X -valley-related donor states in the AlAs barrier of the RTD. In fact, unlike the double-barrier potential profile for the Γ -valley electrons, in GaAs/AlAs RTD's the X valley has a double-well form. Resonant tunneling through the 2D X -valley-related states in AlAs was observed in Ref. 15. The transmission probability through X -valley-related impurity states should be comparable with that through the X -valley QW ground state due to a significant contribution of the Γ -valley wave function to the wave function of the X -valley-related donor state. It is of particular importance that X -valley impurity-related tunneling channels can provide the current peaks at quite low voltage, since the energy difference between the bottoms of the Γ band in GaAs and the X band in AlAs is only 120 meV,¹⁶ and the binding energy of X -valley-

TABLE I. Epitaxial layer structure for the GaAs/AlAs double-barrier diodes.

RTD1	RTD2
	GaAs, $3 \times 10^{18} \text{ cm}^{-3}$, 50 nm
	GaAs, $1 \times 10^{17} \text{ cm}^{-3}$, 70 nm
	GaAs, undoped 2 nm
	AlAs, undoped, 1.7 nm
	GaAs, undoped, 5.6 nm
	AlAs, undoped, 1.7 nm
	GaAs, undoped, 10 nm
	GaAs, $1 \times 10^{16} \text{ cm}^{-3}$, $1 \mu\text{m}$
	GaAs, $3 \times 10^{18} \text{ cm}^{-3}$, $1 \mu\text{m}$
	Substrate: n^+ -c-type GaAs, 0.5 mm
GaAs, $1 \times 10^{18} \text{ cm}^{-3}$, 100 nm	
AlAs, undoped, 2 nm	
GaAs, undoped, 4 nm	
AlAs, undoped, 2 nm	
GaAs, undoped, 100 nm	
GaAs, $1 \times 10^{18} \text{ cm}^{-3}$, 100 nm	
Substrate: n^+ -c-type GaAs, 0.5 mm	

related impurities in AlAs is about 100 meV.¹⁷

Below we will present experimental results and our theoretical model, which allows us to describe the observed low-voltage features in the $I(V)$ characteristics as a resonant tunneling current through the X -valley-related impurity states. Briefly speaking, there are two important facts proving our idea about the origin of the impurity states. First, the localization length of these states, obtained from magnetotransport experiments, is very small. Second, our estimations of the tunneling rates from X donors to emitter and collector contacts are in good agreement with the measured values of the current and with the observation of the effect of an intrinsic bistability in the impurity-assisted current peaks.

Like the authors of Ref. 12, we observed Zeeman splitting of the impurity-assisted current peaks. However, in our case the splitting demonstrates interesting nonlinear behavior as a function of the applied magnetic field. This can be explained by a complex nature of the X -valley-related impurity confinement in GaAs/AlAs RTD's and by an interband mixing controlled by the magnetic field.

EXPERIMENTAL RESULTS

We performed measurements of the current-voltage $I(V)$ characteristics of the RTD's grown by molecular beam epitaxy (MBE) at 550 °C with a growth rate 0.8–1 $\mu\text{m/h}$. The layer sequences for both RTD's are presented in Table I. Both RTD's contain two AlAs barriers and they are characterized by the strongly asymmetrical doping profiles in the different contact layers. The doping asymmetry of the RTD's allows us to compare the tunneling of electrons from the emitter side that contains more impurity centers with the process in the opposite current direction.

The most interesting results were obtained for RTD1, which has only one undoped spacer layer with a thickness of 100 nm, which separates the first barrier region from the highly doped emitter region (doping concentration 10^{18} cm^{-3}). The second barrier is adjacent to the heavily doped layer. RTD2 has a more complex spacer layers composition with two undoped spacer regions (2 and 10 nm) adjacent to the barriers. The spacer regions prevent strong doping of the AlAs barriers and RTD2 does not demonstrate well-resolved prethreshold peaks. The RTD mesas for both structures were fabricated by photolithography and wet chemical etching with mesa dimensions of 16×16 , 8×8 , and $4 \times 4 \mu\text{m}^2$. Standard Ohmic Au-Ge-Ni contacts were al-

loyed to the heavily doped GaAs contact regions. $I(V)$ characteristics were measured in a wide temperature range. At a temperature of 30 mK the $I(V)$ characteristics were measured in an Oxford TLM 400 cryostat with magnetic fields up to 13 T perpendicular and parallel to the current direction. Furthermore, we will concentrate on the results for RTD1, which contains more peculiarities compared to those for RTD2 due to the larger asymmetry in the impurity redistribution. Taking into account growth conditions and structure design, we could expect a considerable concentration of Si atoms inside the AlAs barrier adjacent to the heavily doped GaAs layer of RTD1. Simple calculations according to Ref. 18 with a diffusion coefficient of Si in $\text{Al}_x\text{Ga}_{1-x}\text{As}$ show that the diffusion length in this case equals 2 nm and the average concentration of Si should be in the range 10^{16} – 10^{17} cm^{-3} . Uncertainty arises due to the fact that we do not know exactly the diffusion coefficient of Si in AlAs. It should be likely that the diffusion of Si in AlAs is even larger than in $\text{Al}_x\text{Ga}_{1-x}\text{As}$. Moreover, we do not know the strength of the effect of the AlAs/GaAs interface on Si segregation. On the other hand, the existence of spacer layers considerably prevents penetration of Si atoms into the second barrier due to the low diffusion coefficient of Si in GaAs at 550 °C.¹⁹ The same calculations show that Si concentration inside the AlAs barrier does not exceed the background concentration of 10^{14} cm^{-3} even in the case of 2 nm spacer thickness.

Typical $I(V)$ characteristics are shown in Fig. 1. The forward bias corresponds to the case where electrons tunnel from the wide spacer layer side. First, we briefly consider the high-voltage region, where electrons tunnel through the usual quasibound states of the QW [Fig. 1(a)]. The first and second resonant peaks in the forward and the reverse $I(V)$ characteristics appear as a result of 3D electrons tunneling⁴ from the highly doped emitter through two energy levels of the QW. The energy positions of these levels were calculated to be 180 and 680 meV. The third peak at forward bias is due to the tunneling of 2D electrons, energetically well separated at high voltages from the 3D-emitter carriers and thermalized in the accumulation region in front of the emitter barrier. This conclusion is supported by the observation of the quantum interference of ballistic electrons for the first and second main peaks at both bias polarities.⁴ In the voltage region of the second main resonant peak we find a wide hysteresis

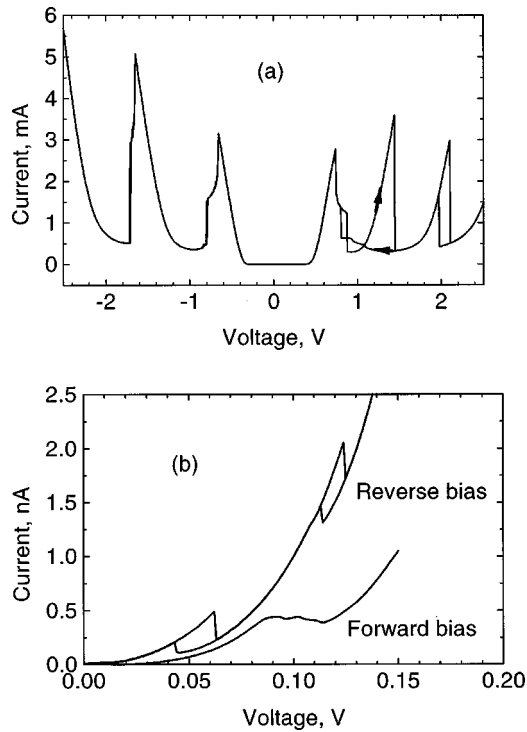


FIG. 1. $I(V)$ characteristics of RTD1 measured at a temperature of 4.2 K: (a) for the voltage range of the main resonance peaks; (b) in the prethreshold voltage range.

loop that can be attributed to the carrier accumulation in the spacer region near the emitter barrier.⁷ The accumulation effect is responsible for changes in the potential profile of our structure leading to a significant redistribution of the electric field along the RTD. As a result, the voltage peak position of the first resonant peak in our asymmetric structure does not differ considerably for both bias polarities.

Remarkable features have been measured in the prethreshold voltage region [Fig. 1(b)]. A steplike fine structure has been observed at forward bias while sawtoothlike peaks are found at reverse bias. The voltage positions of the resonance are different for both polarities. At this very low voltage we observed bistability in sawtoothlike resonances at reverse bias. A similar bistability effect was frequently observed in the case of conventional resonant tunneling, but, to the best of our knowledge, it was never registered in the case of impurity-assisted resonant tunneling. It is known that the reason for the intrinsic bistability is the accumulation of the resonant electrons, which gives rise to the redistribution of the electric field in the system and a simultaneous change of the conditions of tunneling. To achieve the pronounced bistability, the large degree of asymmetry of the tunneling probabilities from the resonant state to the emitter and to the collector is needed.²⁰ In our case, this asymmetry is obviously provided by the doping asymmetry, resulting in the strongly nonuniform distribution of the impurity atoms along the structure. At 30 mK, for the first peak the bistability region extends over 19 mV compared with only 12 mV for the second peak. The bistability demonstrates apparent sensitivity to the sample temperature (Fig. 2). The hysteresis loop shrinks with increasing temperature and finally vanishes at 30 K for the second peak and at 47 K for the first peak. The dependence of the bistability loop width for both peaks

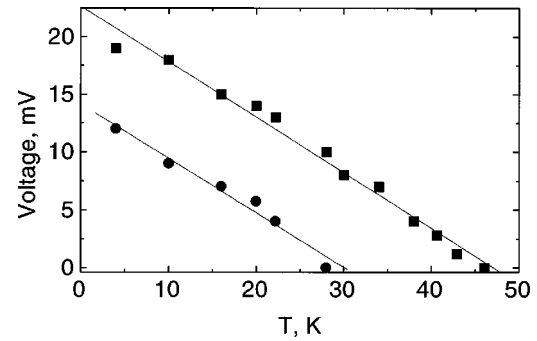


FIG. 2. Temperature dependence of the hysteresis loop width for the first and second prethreshold peaks observed at reverse voltage bias for RTD1.

on temperature shows approximately linear behavior with an equal slope for both curves. The voltage peak position shifts to lower voltages with increasing temperature and decreasing bistability loop. Such a behavior is due to the decrease of the charge accumulation on the resonant states with increasing temperature. The fact that we observe bistable behavior in only one current direction along with its temperature dependencies confirms the intrinsic origin of the observed bistability.

In order to obtain more information about the energy position of the quantum states that are responsible for the prethreshold current peaks, we performed $I(V)$ measurements in high magnetic fields. A magnetic field applied parallel to the electric current considerably modifies the structure of the current peaks. Results at reverse bias for magnetic fields parallel to the current direction are presented in Fig. 3(a). The first peak shifts to lower voltages with increasing B and disappears at $B = 10$ T. The width of the hysteresis loop (not shown here) increases with increasing magnetic field up to the fields of 7 T, in accordance with previously reported behavior for the bistability effect for conventional resonant tunneling,⁷ which is the result of an increase in the charge buildup. In our structure the first peak amplitude becomes smaller with further increasing magnetic field; eventually, the peak disappears at $B = 10$ T. In this case we observed a decrease of the width of the hysteresis loop in a number of magnetic fields.

The forward bias current-voltage characteristics are shown in Fig. 3(b) for several values of magnetic field B in the voltage range of the first step. One can see that the application of a magnetic field leads to substantial narrowing of the prethreshold peaks. Analogous behavior can be observed at a magnetic field perpendicular to the current.

A magnetic field applied perpendicular to the current direction leads to a splitting of the prethreshold peaks. The effect becomes measurable at magnetic fields above 5 T, especially at forward bias (Fig. 4). The splitting shows an unusual behavior. It only displays a linear dependence on B in the region of high magnetic fields. Surprisingly, in the magnetic field range from 5 to 7 T the distance between the two current maxima begins to decrease instead of the expected increase. The dependence of the splitting voltage on B is shown in Fig. 5. We attribute the splitting at high magnetic fields to the Zeeman effect. In this range of magnetic fields the splitting increases linearly with B , as was expected for the energy splitting of two different spin states.

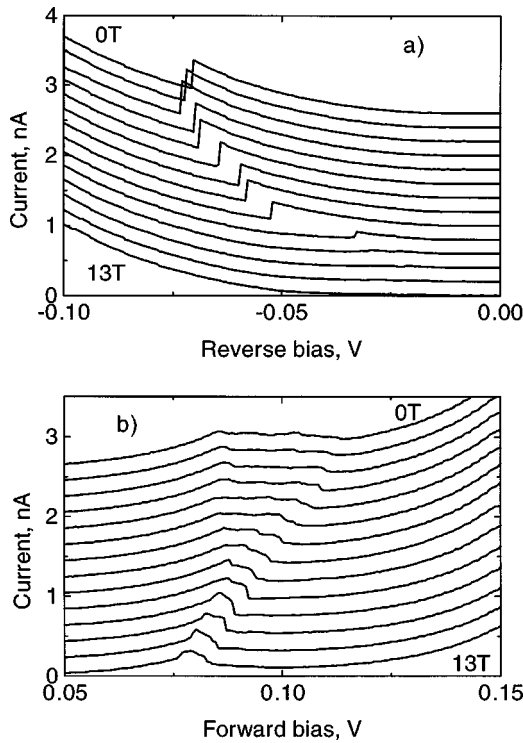


FIG. 3. $I(V)$ characteristics of RTD1 measured at 30 mK at (a) reverse and (b) forward voltage biases in the region of the first prethreshold resonance with increasing magnetic field B_{\parallel} with a 1-T step. The curves are vertically offset for clarity.

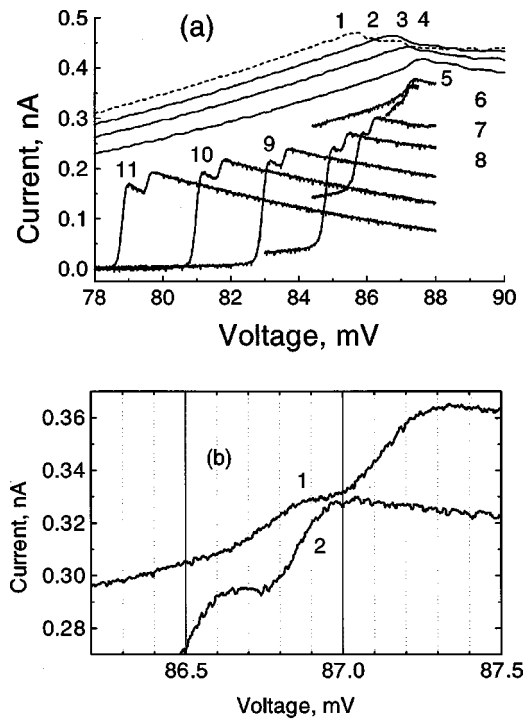


FIG. 4. $I(V)$ characteristics of RTD1 measured at 30 mK at forward voltage bias in the region of the first prethreshold resonance at magnetic fields perpendicular to the current direction: (a) B_{\perp} : 1, 0 T (dashed); 2, 2 T; 3, 3 T; 4, 4 T; 5, 5 T; 6, 5.4 T; 7, 7.5 T; 8, 9.5 T; 9, 11 T; 10, 12 T; 11, 13 T; (b) B_{\perp} : 1, 5.4 T; 2, 6.4 T.

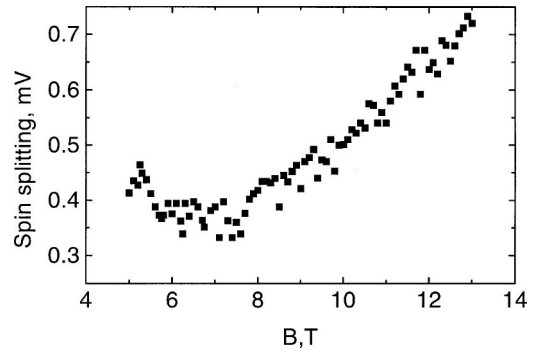


FIG. 5. Spin splitting of the first step on $I(V)$ characteristics of RTD1 measured at forward voltage bias.

The second peak shows a shift in the opposite direction with respect to the first one with increasing magnetic field (Fig. 6). This reflects different degrees of wave-function localization of the corresponding states.

THEORETICAL MODEL AND DISCUSSION

Prethreshold current peaks and steps were observed in our RTD at very low voltages. In order to find the energy of the states that are responsible for the observed resonant tunneling one should calculate the scaling factor that determines the relation between the voltage and energy units. Since the steps and peaks are strongly broadened we cannot employ the method described in Ref. 12, which is based on the analysis of peak smoothing, because of the considerable broadening of the peaks, most probably due to strong dispersion of the impurity-atom position. We have determined the scaling factor using the onset voltage V_s for the first main resonance of RTD1. At this voltage the Fermi energy in the 3D emitter (55 meV for emitter doping concentration) coincides with the energy of the ground state in the QW (180 meV). This method provides a scaling factor of 0.35. Therefore, the energy position of the first impurity-related level at forward bias is about 150–160 meV below the 2D level of the QW of GaAs. This value is much larger than that predicted for a single isolated hydrogenic donor in a GaAs quantum well, which is of the order of 20 meV.⁹ Moreover, we obtain a very small localization size of the states responsible for prethreshold peaks from magnetotunneling mea-

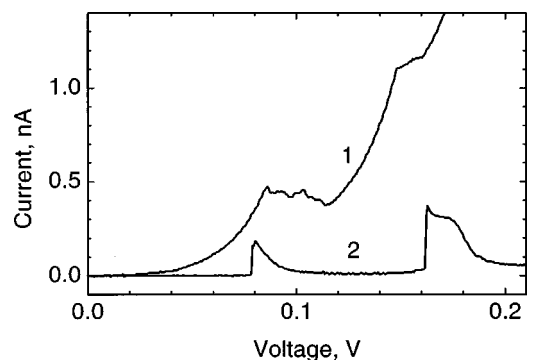


FIG. 6. $I(V)$ characteristics of RTD1 measured at 30 mK under forward bias in the voltage range between the first and second prethreshold peak (1) without and (2) with a magnetic field of 13 T applied perpendicular to the current direction.

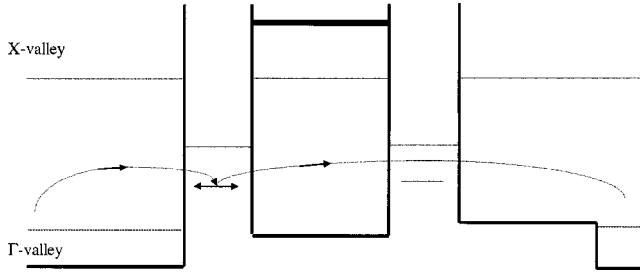


FIG. 7. Schematic representation of the conduction-band minima at the Γ (full line) and X (dashed line) points of the Brillouin zone of a GaAs/AlAs structure corresponding to RTD1, shown below the first quantum-size level of the GaAs QW.

surements. An estimation for the localization length can be obtained from the diamagnetic shift of the first peak in the $I(V)$ characteristic in magnetic fields both parallel and perpendicular to the current direction. The diamagnetic shift is different for 3D emitter states compared to that of impurity states. With increasing magnetic field the binding energy corresponded to the first resonance increases. The difference in the binding energies at a certain value of B and $B=0$ can be estimated as

$$\Delta E = e^2 \langle z^2 \rangle B^2 / (2m^*), \quad (1)$$

where e is the electron charge, $\langle z^2 \rangle$ is the mean square expectation value for the wave function in the plane perpendicular to the applied magnetic field, and m^* is the effective mass. This gives us a value of $\Delta z \approx \sqrt{\langle z^2 \rangle} \approx 4$ nm for the localization length of the resonant state causing the first step at forward bias. The values of size localization obtained for other resonant peaks are of the same order. Thus, the states responsible for the prethreshold peaks are localized more strongly than the hydrogenic donors in the GaAs QW.

We believe that the registered impurity states should be attributed to the donor-related states of the X valley in the conduction band of the AlAs barrier layer. Indeed, as will be shown below, the estimated tunneling rate and value of the impurity-related current in our model are in good agreement with the observed experimental results and the observed bistability effect.

In AlAs the conduction-band minimum of the X valley lies 120 meV higher¹⁶ than the bottom of the Γ valley of GaAs. As a result, for X electrons in our structure we have a double-well potential profile, in contrast to a double-barrier profile for Γ electrons (see Fig. 7, where the potential profile in the system is shown schematically). Γ electrons from the heavily doped emitter region can tunnel via states of the X valley due to a Γ - X mixing at the heterointerface. Impurity atoms can provide impurity-assisted tunneling current peaks at very low voltage because of the relatively small height of the Γ - X barrier at the GaAs-AlAs interface, as well as the large binding energy of X -valley-related Si donor states in AlAs (about 100 meV).¹⁷

It is well known that the degeneracy of the impurity states in semiconductors with X minima of the conduction band is partially canceled due to the so-called valley-orbit interaction. As was shown in Ref. 21, the valley-orbit splitting of the Si donor states in AlAs is quite small. However, in our RTD we have other reasons that result in the appearance of

energetically well-separated donor levels. The first reason is strain of the AlAs layer due to the small lattice misfit in RTD's grown by MBE. As a result of this deformation, the energy of the X valley, oriented along the growth direction (X_z valley), shifts upwards with respect to that of the valleys oriented along the layers (X_{xy} valleys). The value of this energy shift is about 20 meV.²² However, in our RTD the bottom of the X_{xy} valleys is shifted considerably due to the strong quantization in thin AlAs wells. The quantization energy is roughly inversely proportional to that component of the electron effective mass responsible for the electron motion perpendicular to the layers. This value is equal to $0.19m_0$ for X_{xy} valleys and $1.1m_0$ for X_z valleys.²³ Based on these data, we found that the quantization in the AlAs causes a shift of the X_{xy} valley bottom of about 60 meV above the X_z -valley bottom. This shift is substantially higher than that due to the deformation. As a result, the X_{xy} valley lies higher than the X_z valley. Consequently, we assume that the energetic position of the donor states, related to the different valleys, has the same order as the valley bottoms. Note that this situation is different from that reported in Ref. 24, where a single-barrier tunneling structure was studied. In that work quantization is negligible due to the relatively thick AlAs layers, and the bottom of the X_z valley is higher than the bottom of the X_{xy} valley.

The proposed origin of the registered impurity states is also consistent with the observation of the intrinsic bistability of the impurity-assisted current peaks. In our RTD the density of impurity states is high in only one AlAs barrier, which is not separated from the contacts by a spacer. This explains the observation of bistability for tunneling via these impurity states at reverse voltage bias and the absence of a bistability effect at forward bias.

As we mentioned previously, the bistability in the RTD arises due to the charge buildup of the resonant electrons and related perturbation of the potential profile in the structure. An accumulation of the electrons in the impurity states in the GaAs QW is unlikely to occur because the probabilities of their tunneling to the emitter and collector through the similar AlAs barriers are of the same order. In contrast, accumulation can be realized in the case of tunneling through the X -valley-related impurities. The Si impurity atoms are mainly localized in the AlAs barrier close to the heavily doped spacerless GaAs contact. The rate of the tunneling of the electrons from the spacerless contact to the impurity is solely determined by the Γ - X mixing. In contrast, the rate of tunneling of the electrons from the impurity states to the other side of the structure is relatively low. The latter is due to the weak overlap of the electron wave functions corresponding to the states localized in the contact with spacer and in impurity states. As a result, at reverse bias considerable accumulation of electrons on the impurity states in AlAs occurs. The hysteresis disappears for the second peak at 30 K, but can still be observed for the first peak up to a temperature of 47 K in good agreement with the larger binding energy for the first peak. The linear dependencies with the same slope of bistability width, shown in Fig. 2, demonstrate that the redistribution of the electric field in a low voltage range does not change considerably and the calculated scaling factor is approximately the same for the prethreshold voltage range. In the case of forward voltage bias, the charge

buildup in the second barrier with large donor concentration is small since the electron can easily tunnel to the collector.

It is worth noting that the physical picture of the observed impurity-related bistability is more complicated than that in the case of conventional resonant tunneling. In particular, since we deal with the tunneling from 3D emitter states to the 0D states in the AIAs layer and vice versa, there is no in-plane momentum-conservation requirement, and the probability of tunneling is determined by the *total* energy of the electrons and the in-plane electron wave vector. This should essentially modify the dependence of the tunneling current on the position of the impurity levels with respect to the bottom of the emitter conduction band.

In order to support our hypothesis about the origin of the observed low-voltage current peaks, we made a rough estimate of the current value due to the tunneling through the X -related donor states of AIAs. The current is determined by the impurity concentration in the barrier region and the time needed for an electron to tunnel from an emitter state through a solitary X -valley-related donor impurity state to a Γ -related collector state.

The tunneling from the impurity states to the spacerless contact is much faster than that to the contact with a spacer due to the low transparency of the X -valley-related barrier of the GaAs layer. Hence, the impurity-assisted current is mainly determined by the tunneling rate from the X -valley-related donor state to the contact with spacer. To calculate this value, we follow the phenomenological approach of Liu.²⁵ We calculated the tunneling rate in question with the use of the perturbation theory, assuming the Γ - X mixing terms as a perturbation. The penetration of the X -valley-related donor states over the relatively thick GaAs layer is much weaker than the penetration of Γ -valley-related electron state localized in contact with spacer states over the AIAs layer. This is because the Γ -valley effective mass of GaAs is considerably less than the X -valley effective mass of AIAs. Therefore, the tunneling rate is determined by the overlap of the wave function of the collector state and the donor state wave functions on the interface between the AIAs and the GaAs layer, integrated over the interface.

For rough estimates we used the wave functions of bulk donor states, obtained in Ref. 26 with the use of the variational method, and obtained the tunneling rate $2 \times 10^6 \text{ s}^{-1}$ for the X_z -valley-related donor states. The obtained rate is consistent with the measured current value if the volume concentration of donors in the barrier is of the order 10^{16} cm^{-3} . Note, however, that the value of the coefficient characterizing the strength of the Γ - X mixing is most probably overestimated in Ref. 25, since in that paper the barrier between the Γ -valley bottom of GaAs and the X -valley bottom of AIAs was assumed to be 190 meV, while it is now believed to be 120 meV.¹⁶ This means that the given value of the donor concentration is underestimated. For more rigorous calculations of the tunneling rate it is necessary to take into account the finite contribution of the Γ -valley states to the donor wave functions, as well as their modification due to the quantization effect in the AIAs layer.

Now we can justify the binding energy of the donor-related impurity states with respect to the X -valley minimum in the AIAs layer. We find that these energies are 20–30 meV above the conduction-band minimum of GaAs. The

X -valley band in AIAs is 120 meV above the conduction-band minimum of the Γ valley adjacent to the GaAs layer and the binding energy of X donors is 80–90 meV. The values are consistent with those reported in the literature.^{17,27} The energy position of the second resonant state is about 60–70 meV, which can be explained by the quantization of the X_{xy} -valley-related states in AIAs.

The behavior of the impurity-assisted current peaks in magnetic fields can be qualitatively explained within the framework of the proposed model. The shift of the impurity levels in magnetic fields is roughly inversely proportional to the component of the electron effective mass, which is responsible for the motion of the electron in the plane perpendicular to the magnetic field, and also depends on the spatial localization of the wave function. The different shifts of the first and second peaks with increasing magnetic field, Fig. 6, can be explained by the different values of the effective masses in question, as well as by the different lateral localization of the corresponding wave functions.

The magnetic length L_B is determined by the equation

$$L_B = [h/(2\pi eB)]^{1/2}. \quad (2)$$

At a relatively low magnetic field of $B < 5 \text{ T}$, the magnetic length is $L_B \approx 12 \text{ nm}$, which is larger than the localization length of the impurity-state wave function. At these magnetic fields we observed a small change of the peak position and amplitude. In high magnetic fields the changes become drastic, because the application of the magnetic field substantially modifies the localization of the electron wave function. This can be responsible for the disappearance of the lowest peak at reverse bias with increasing magnetic field [Fig. 3(a)].

Another experimental finding for RTD 1 is the observation of the splitting of the first impurity-related peak into the two well-defined peaks in magnetic fields perpendicular to the current direction. The splitting of the peak shows an unusual dependence on the magnetic field. It shows linear behavior only in the region of high magnetic fields (Fig. 5). We attribute the splitting of the impurity-assisted peaks in magnetic fields at forward bias to the Zeeman splitting of the energy levels corresponding to the different spin states of the electron localized on an impurity. The energy splitting is equal to $g\mu_B B$, where μ_B is the Bohr magneton and g is the impurity g factor. Because of that, the measurement of the slope of the dependence of the voltage splitting on the value of the magnetic field provides valuable information about the impurity g factor.

We determined the g factor for the impurity from a linear extrapolation of the high-magnetic-field dependence to $V = 0$ at $B = 0$ with a slope of $g\mu_B/\alpha$, where α is the scaling factor. Using a scaling factor of 0.35 as determined from the onset voltage, we obtained a g factor value of about 0.34 ± 0.05 for the region of high magnetic fields. This value is quite different from that for the X -valley electrons in a GaAs/AIAs superlattice structure,²⁸ which was reported to be 1.97. This disagreement can be due to the complex nature of the investigated impurity states. It is known that in crystals the g factor of electrons is different from that in the free space due to the interband interaction.²⁹ In low-dimensional heterostructures the value of the g factor is modified, since the electron wave function contains the contributions belonging

to the different materials. In particular, this gives rise to the dependence of the electron g factor of 2D electrons on the QW width.³⁰ In our RTD a similar effect can take place due to the partial contribution of Γ and X states of GaAs to the impurity-state wave function.

Since the application of the magnetic field modifies the electron confinement, a nonlinear dependence of the spin splitting on the magnetic field can be manifested. This was demonstrated both theoretically and experimentally for exciton states.^{31,32} The features described are in qualitative agreement with our results on spin splitting. For more accurate conclusions about the structure of the observed impurity states and their modification in strong magnetic fields the development of a sophisticated theory is necessary.

CONCLUSION

In conclusion, we observed the prethreshold current peaks due to resonant tunneling through the X -valley-related impurity states of the AlAs barrier of GaAs/AlAs resonant tunnel-

ing structures. Asymmetry in the doping profile of the structure under investigation provides substantial charge accumulation at one of the bias polarities, which gives rise to the intrinsic bistability of the current-voltage characteristic. The value of the current, obtained using a perturbation theory approach, is in good agreement with the experimental data. The effective Zeeman spin splitting factor is determined for AlAs/GaAs RTD's and its value is equal to 0.34 ± 0.05 . The unusual nonlinear dependence of the effective magnetic spin splitting observed for magnetic fields in the range from 5 to 7 T reflects the complex interband mixing effects that occur in strong magnetic fields.

ACKNOWLEDGMENTS

We are grateful to L. N. Kravchenko for providing the resonant tunneling heterostructures. One of us (S.A.V.) would like to acknowledge support by the Alexander von Humboldt Foundation.

*On leave from the Institute of Semiconductor Physics, National Academy of Sciences of Ukraine, Kiev 252028, Ukraine.

¹L. L. Chang, L. Esaki, and R. Tsu, *Appl. Phys. Lett.* **24**, 593 (1974).

²V. J. Goldman, D. C. Tsui, and J. E. Conningham, *Phys. Rev. B* **36**, 7635 (1987).

³C. Zhang, M. L. F. Lerch, A. D. Martin, P. E. Simmonds, and L. Eaves, *Phys. Rev. Lett.* **72**, 3397 (1994).

⁴A. E. Belyaev, S. A. Vitusevich, T. Figielski, B. A. Glavin, R. V. Konakova, L. N. Kravchenko, A. Makosa, and T. Wosinski, *Surf. Sci.* **361/362**, 235 (1996).

⁵V. J. Goldman, D. C. Tsui, and J. E. Conningham, *Phys. Rev. Lett.* **58**, 1256 (1987).

⁶L. Eaves, G. A. Toombs, F. N. Sheard, C. A. Payling, M. L. Leadbeater, E. S. Alves, T. J. Foster, P. E. Simmonds, M. Henini, and O. H. Hughes, *Appl. Phys. Lett.* **52**, 212 (1988).

⁷A. E. Belyaev, S. A. Vitusevich, B. A. Glavin, R. V. Konakova, T. Figielski, A. Makosa, L. N. Kravchenko, and W. Dobrovolski, *Inorg. Mater. (Transl. of Neorg. Mater.)* **33**, 116 (1997).

⁸M. W. Dellow, P. H. Beton, C. J. G. M. Langerak, T. J. Foster, P. C. Main, L. Eaves, M. Henini, S. P. Beaumont, and C. D. W. Wilkinson, *Phys. Rev. Lett.* **68**, 1754 (1992).

⁹R. L. Greene and K. K. Bajaj, *Phys. Rev. B* **31**, 913 (1985).

¹⁰J. W. Sakai, P. C. Main, P. H. Beton, N. La Scala, Jr., A. K. Geim, L. Eaves, and M. Henini, *Appl. Phys. Lett.* **64**, 2563 (1994).

¹¹J.-W. Sakai, T. M. Fromhold, P. H. Beton, L. Eaves, M. Henini, P. C. Main, F. W. Sheard, and G. Hill, *Phys. Rev. B* **48**, 5664 (1993).

¹²M. R. Deshpande, J. W. Sleight, M. A. Reed, R. G. Wheeler, and R. J. Matyi, *Phys. Rev. Lett.* **76**, 1328 (1996).

¹³A. K. Geim, T. J. Foster, A. Nogaret, N. Mori, P. J. McDonnell, N. La Scala, Jr., P. C. Main, and L. Eaves, *Phys. Rev. B* **50**, 8074 (1994).

¹⁴M. R. Deshpande, E. S. Hornbeck, P. Kozodoy, N. H. Dekker, J.

W. Sleight, M. A. Reed, C. L. Fernando, and W. R. Frensley, *Semicond. Sci. Technol.* **9**, 1919 (1994).

¹⁵E. E. Mendez, E. Calleja, C. E. T. Goncalves da Silva, L. L. Chang, and W. I. Wang, *Phys. Rev. B* **33**, 7368 (1986).

¹⁶R. Teissier, J. J. Finley, M. S. Skolnick, J. W. Cockburn, J.-L. Pelouard, R. Grey, G. Hill, M. A. Pate, and R. Planel, *Phys. Rev. B* **54**, R8329 (1996).

¹⁷S. T. Lee, A. Petrou, M. Dutta, J. Pamulapati, P. G. Newman, and L. P. Fu, *Phys. Rev. B* **51**, 1942 (1995).

¹⁸E. F. Schubert, C. W. Tu, R. F. Kopf, J. M. Kuo, and L. M. Lunardi, *Appl. Phys. Lett.* **54**, 2592 (1989).

¹⁹E. F. Schubert, *J. Vac. Sci. Technol. A* **8**, 2980 (1990).

²⁰M. L. Leadbeater, E. S. Alves, L. Eaves, M. Henini, O. H. Hughes, F. W. Sheard, and G. A. Toombs, *Semicond. Sci. Technol.* **3**, 1060 (1988).

²¹E. R. Glaser, T. A. Kennedy, B. Molnar, R. S. Sillmon, M. G. Spencer, M. Mizuta, and T. F. Kuech, *Phys. Rev. B* **43**, 14 540 (1991).

²²P. Dawson, C. T. Foxon, and H. W. van Kesteren, *Semicond. Sci. Technol.* **5**, 54 (1990).

²³S. Adachi, *J. Appl. Phys.* **58**, R1 (1985).

²⁴I. E. Itskevich, L. Eaves, P. C. Main, M. Henini, and G. Hill, *Phys. Rev. B* **57**, 7214 (1998).

²⁵H. C. Liu, *Appl. Phys. Lett.* **51**, 1019 (1987).

²⁶W. Kohn and J. M. Luttinger, *Phys. Rev.* **98**, 915 (1955).

²⁷G. Weber, *Appl. Phys. Lett.* **67**, 1447 (1995).

²⁸H. W. van Kesteren, E. C. Cosman, W. A. J. A. van der Poel, and C. T. Foxon, *Phys. Rev. B* **41**, 5283 (1990).

²⁹A. A. Kiselev, E. L. Ivchenko, and U. Rössler, *Phys. Rev. B* **58**, 16 353 (1998).

³⁰M. J. Snelling, G. P. Flinn, A. S. Plaut, R. T. Harley, A. C. Tropper, R. Eccleston, and C. C. Phyllips, *Phys. Rev. B* **44**, 11 345 (1991).

³¹G. E. W. Bauer and A. Ando, *Phys. Rev. B* **37**, 3130 (1988).

³²W. Ossau, B. Jakel, E. Banger, G. Landwehr, and G. Weimann, *Surf. Sci.* **174**, 188 (1986).